Per. Mineral. (2007), 76, 2-3, 5-24 doi:10.2451/2007PM0015
SPECIAL ISSUE: In honour of Ezio Callegari on his retirement http://go.to/permin

PERIODICO di MINERALOGIA
established in 1930

An International Journal of
MINERALOGY, CRYSTALLOGRAPHY, GEOCHEMISTRY, ORE DEPOSITS, PETROLOGY, VOLCANOLOGY
and applied topics on *Environment*, *Archaeometry* and *Cultural Heritage*

Petrography and thermobarometry of high-pressure ultramafic ejecta from Mount Vesuvius, Italy: inferences on the deep feeding system

CORRADO CIGOLINI *

Dipartimento di Scienze Mineralogiche e Petrologiche, Università degli Studi di Torino,
Via Valperga Caluso, 35, 10125 Torino, Italy

ABSTRACT. — Ultramafic ejecta preserved as xenoliths in 1906 pyroclastic deposits of Mount Vesuvius are essentially clinopyroxene-bearing dunites and clinopyroxenites. Some have been tectonized and exhibit mosaic-equigranular and porphyroclastic textures typical of mantle peridotites. Dunites show a orthocumulate-heterogranular texture consisting of euhedral to subeuhedral olivine (Fo_{90-88}), locally coexisting with greenish pyroxene of diopsidic composition, and interstitial yellowish glass essentially of phono-tephritic composition (Mg# 48-62). Few large crystals of forsteritic olivine may show deformation bands ("strain lamellae") and twinning as well as decompression textures that reflect a deep environment of formation. Some olivine clots exhibit abundant microinclusions of Cr-spinel (Cr-hercynite and chromite) and deep brownish to clear glass. Primitive liquids included in forsteritic olivine have a trachybasaltic composition (Mg# up to 71-75). Locally, microinclusions of phlogopite are coexisting with glasses of phono-tephritic and basaltic trachy-andesitic composition (Mg# ranging 29-65). A late, acicular, seldom radiating brown-greenish clinopyroxene of salitic composition may form around large olivine crystals and coexists with minute secondary olivine (Fo_{86-85}), plagioclase (An_{78-76}) and rarely leucite.

Thermobarometric estimates obtained by means of a grid of selected reactions indicate that dunitic materials equilibrate with primitive, moderately hydrous trachybasaltic melts (1.5-2.5 wt% H_2O) at ~12.4-13 kbar for temperatures ranging 1250-1300°C. Equilibration occurs in proximity and/or below the crust-mantle transition, located at a depth of 30-36 km below Mount Vesuvius. More differentiated tephritic melts will react with the ultramafic nodules and equilibrate at about 3 kbar and 1220-1170°C. These regimes constrain a sector of an upper reservoir (whose top is located at about 9-10 km depth) where deep cumulitic materials are momentarily stored before being erupted during paroxysmal eruptions.

RIASSUNTO. — I proietti ultrafemici associati ai depositi piroclastici eruttati dal Vesuvio durante la crisi eruttiva del 1906 sono costituiti da duniti e clinopirosseniti e presentano una tessitura di tipo ortocumulitico localmente eterogranulare. Alcuni campioni presentano una tessitura equigranulare a mosaico e porfiroclastica. I campioni dunitici sono costituiti da olivina idiomorfa e subidiomorfa, localmente inclusa in un pirosseno pecilitico di natura diopsidica su una matrice vetrosa interstiziale. E' presente, inoltre, un pirosseno aciculare più

* E-mail: corrado.cigolini@unito.it

alluminifero che si accresce localmente ai bordi delle olivine in corrispondenza di plaghe vetrose.

Spesso l'olivina presenta microinclusioni di spinelli cromiferi (ercinite e cromite) e, più raramente, di vetro, occasionalmente associato a flogopite. Le microinclusioni vetrose (prive di flogopite) sono costituite da un vetro di composizione trachibasaltica (avente numero Mg# compreso tra 71 e 75), mentre il vetro associato alla mica presenta una composizione fonotefritica e trachiandesitica (Mg# compreso tra 29 e 65). Inoltre il vetro interstiziale, presente nella matrice, è essenzialmente di composizione fonotefritica passante a trachibasaltica (Mg# 48-62).

Le stime termobarometriche ottenute su equilibri solido-liquido suggeriscono che i cumulati dunitici si siano formati in una camera magmatica a temperature intorno a 1250-1300 °C e pressioni di 12,4-13 kbar. Dette stime sono confrontabili con i dati geofisici relativi alla transizione crosta-mantello localizzata, in corrispondenza del Vesuvio, a circa 30-36 km di profondità.

In fase di risalita e stazionamento i fusi più differenziati di composizione tefritica reagiscono con gli xenoliti ultrafemici e si equilibrano a pressioni di circa 3 kbar e temperature di 1220-1170 °C. Questi regimi termobarometrici sono in buon accordo con l'esistenza di un settore di camera magmatica situato a circa 9-10 km di profondità. In questa regione i materiali di origine profonda stazionano prima di essere eruttati durante le fasi parossistiche.

KEY WORDS: *Ultramafic ejecta, dunite, clinopyroxenite, thermobarometry, phlogopite microinclusions, magma chamber.*

INTRODUCTION

The petrogenesis of Mount Vesuvius magmas has been a extensively debated during the last century. The early works of Lacroix (1907; 1917), Washington (1906; 1917) and Zambonini (1910) essentially focused on describing the mineralogy and the petrography of rocks of this potassic suite. Few years later, Rittmann (1933) explained the lavas erupted from Somma-Vesuvius (essentially theprite and phonolitic tephrite) as a result of assimilation of dolomite (of the Tertiary basement rocks) by uprising trachytic magmas. This view was challenged by Savelli (1967) who showed, on petrochemical grounds, that this process could not affect such large volumes of magma. However, interactions between the magma and wall-rocks do occur but lead to the genesis of contact-metasomatic skarns in the surrounding of the magma chamber (Barberi and Leoni, 1980; Joron *et al*., 1987; Fulignati *et al*., 2000a). Vesuvian melts and cumulitic nodules from Somma-Vesuvius have been systematically studied by Hermes and Cornell (1981), Cundari (1982), Joron *et al*. (1987). Recent contributions on the 79 A.D. and 1906 eruptions (Santacroce *et al*., 1993; Cioni *et al*., 1995) have also discussed the role of cumulus processes operating within this magmatic system. Pyroclastic deposits of recent Vesuvian eruptions contain abundant cumulitic "clinopyroxenite-mushes", subordinated weherlite and rare dunite.

Hermes and Cornell (1981) concentrated their research on clinopyroxene-rich ejecta and concluded that these materials are essentially related to crystal fractionation occurring within an heterogeneous magma chamber where distinct cumulus processes are effective. In contrast, Cundari (1982) proposed that evolved Vesuvian magmas may originate by interaction of a basanitic melt with cumulitic olivine to give clinopyroxenite together with a phonotephritic melt. Thermometric estimates on fluid inclusions trapped in a variety of cumulitic materials, including metasomatic "skarns", have been given by Belkin *et al*. (1985), Cortini *et al*. (1985), Belkin and De Vivo (1983): homogenisation temperatures for melt inclusions into mineral phases of metasomatic nodules are in the range of 850-1050 °C, whereas in clinopyroxenite they may go up to 1170-1240 °C. These estimates are essentially consistent with those determined by Cioni *et al*. (1995) for melt inclusions found in ferromagnesian minerals of the 79 A.D.. Recent contributions focused on determining the pre-eruptive volatile content of Vesuvian magmas inferred from the data on a variety of melt inclusions found in ferromagnesian mineral phases. In particular, Belkin *et al*. (1998) found H_2O contents ranging 0.6-2.7 wt% in interplinian Vesuvius lavas (erupted before 1631). Moreover, Marianelli *et al*. (1999) measured water contents up to 3.4 wt%, with CO_2 ranging 0.17-0.43 wt% for recent lavas and tephra (erupted in 1906 and 1944). More recently, Fulignati and co-workers (Fulignati *et al*., 2000b) measured (by means of FTIr) the volatile contents of several melt inclusions found in olivine of cumulitic

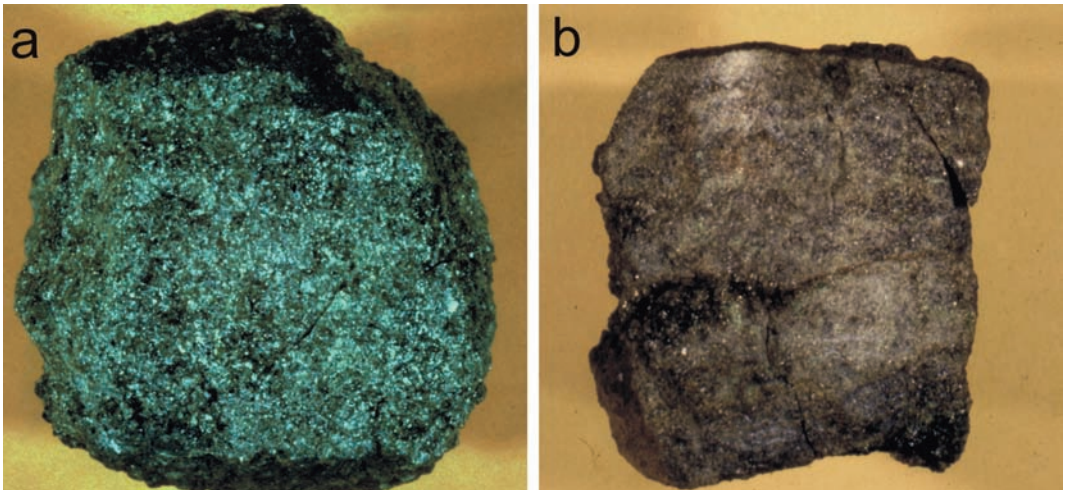

Fig. 1 – (a) Hand specimen of a clinopyroxene-bearing dunite ejecta. The sample is about 6 cm in diameter and shows an outer crust of few mm of clinopyroxenite due to reaction with the host magma. (b) Dunite sample of about 8 cm in length and 10 cm high. Dunite shows a typical "banding" due to abundant Cr-spinel included in olivine and distributed in subhorizontal layers. Olivine of the "main" body of the sample may contain microinclusions of more primitive trachybasaltic melts. Centimetric veinlets and pockets of large, greenish olivine crystals (up to 4 mm in size) are found cross-cutting dunitic ejecta. These olivines may carry microinclusions of Cr-rich phlogopite locally coexisting with glasses of tephritic and phonotephritic composition. The upper rim consists of clinopyroxenite due to reaction with the host magma (sample Vu65 has been extracted from this layer).

dunites ejected in 1944: they found water contents averaging 3.3 wt% coexisting with ~0.2 wt% of CO_2.

On petrogenic grounds, Schiano *et al*. (2004) proposed that primitive melt inclusions of Vesuvius and Phlegraean Fields are related to a common phlogopite-bearing mantle source enriched in incompatible elements carried by water dominated fluids released from the subducting slab. More recently, Di Renzo *et al*. (2007) suggested the possibility that Vesuvian magmas could also be affected by substantial crustal contamination inherited both from the Hercynian basement rocks and/or the Mesozoic limestone, where primitive magma are stored within an active magma chamber located at 8-10 km depth.

A comprehensive review of the evolution and dynamics of Somma-Vesuvius has been recently given by Santactroce *et al*. (2005).

In this work, I will first discuss the petrography and the mineral chemistry of Cr-spinel dunitic ejecta which bear fragments of upper-mantle material likely recycled in a magma reservoir located at the base of the crust (Cigolini, 1997; 1999). I will then refine earlier thermobaromentric estimates on these materials and discuss their environment of formation.

Petrography

Ultramafic ejecta selected for this study are *Cr-spinel dunites* and *clinopyroxenites*. These are associated with the pyroclastic deposits of the 1906 eruption. These samples differ from the dunitic nodules reported by Fulignati *et al*. (2000b) since they carry relict textural features typical of mantle peridotites, together with a rather peculiar mineralogy.

Hand specimens of *dunitic ejecta* are characterised by an heterogranular texture. Sampled nodules are nearly spheroidal in shape with a diameter ranging 3-12 cm (Fig. 1). Olivine makes up to 90 % of the mode and exhibits a white-yellowish color. Outer parts of the samples show a partly oxidized crust consisting essentially of deep green, dimensionally larger, *olivine-bearing clinopyroxenite* (Figs. 1a, 1b). Millimetric to

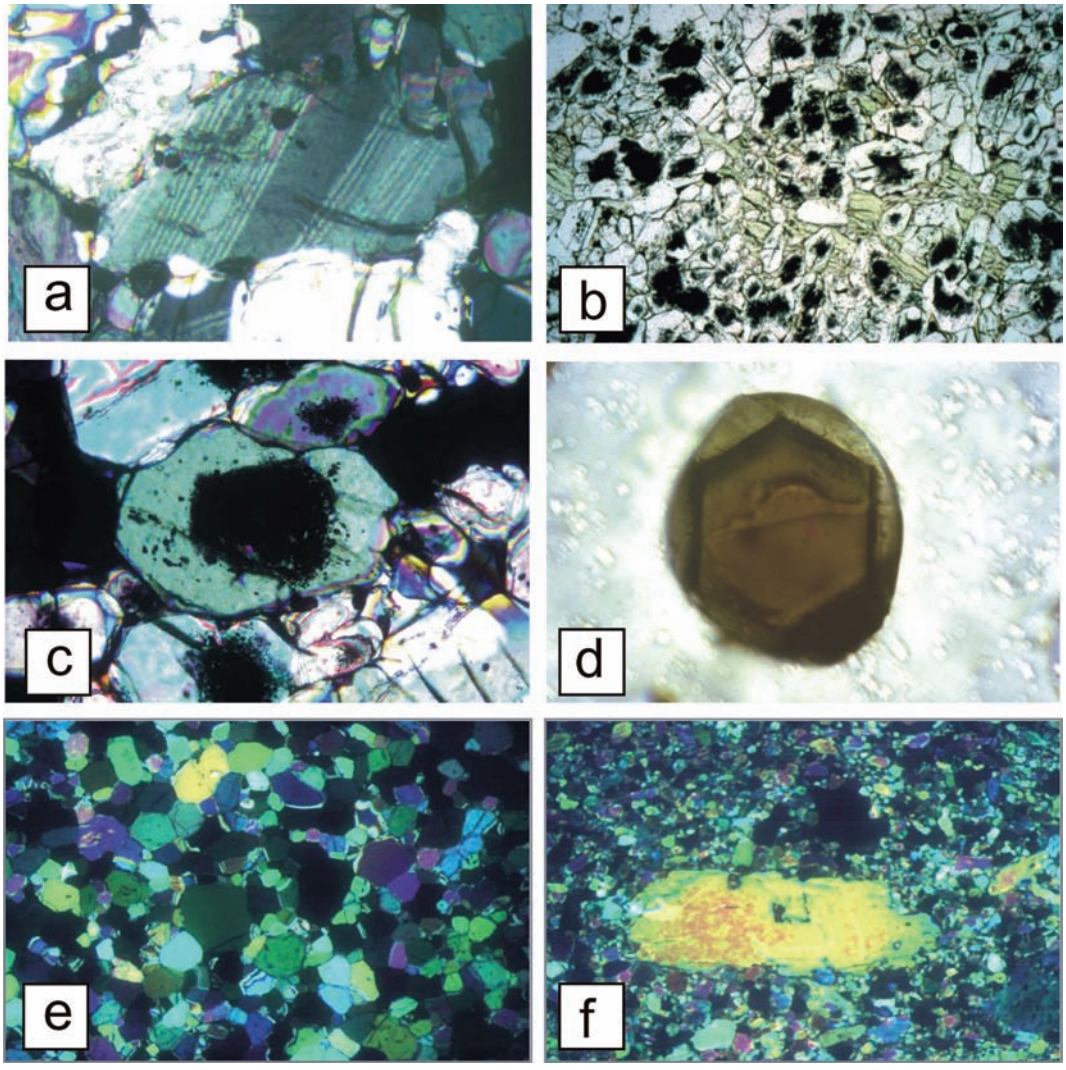

Fig. 2 – Photomicrographs of selected textures and mineral assemblages within dunitic ejecta of Mont Vesuvius. (a) Photomicrographs of deformation twinning within a single olivine crystal. Plane polarised light. Long dimension 1.2 mm. (b) Olivine with opacitic aggregates of Cr-spinels, and interstitial clinopyroxene (greenish). Plane polarised light. Long dimension 4.2 mm. (c) Pseudomorphic Cr-spinel in forsteritic olivine replacing a pre-existing garnet (see text for details). Crossed polarisers. Long dimension 1.2 mm. (d) Photomicrograph of a chromium-rich phlogopite coexisting with glass within an olivine crystal. Plane polarised light. Long dimension 1.2 mm. (e) Mosaic-equigranular texture within a dunitic ejecta. Plane polarised light. Long dimension 4.2 mm; (f) Photomicrograph of a porphyroclastic texture in clinopyroxenite. A clinopyroxene porphyroclast is surrounded by a re-crystallised transitional mosaic-porphyroclastic matrix consisting of the same phase (Sample Vs 100). Crossed polarisers. Long dimension 4.2 mm.

centimetric veinlets and pockets that crosscut some samples consists essentially of larger greenish olivine that may contain abundant microinclusions of brownish glass (Fig. 1b). Nodules of "massive" *clinopyroxenite* are rare and may be found only occasionally. They show relict porphyroclasts of diopsidic pyroxene in a matrix of the same mineral phase. This clinopyroxenite is quite different than the "pyroxene-mush aggregates", consisting of dimensionally larger diopsidic pyroxene wet by an interstitial melt (preserved as glass), described by Santacroce *et al*. (1993).

Most of the sampled dunitic nodules show an *orthocumulate heterogranular* texture consisting essentially of euhedral to subeuhedral clear *olivine* (about 0.2-1.2 mm) of fosteritic composition (Fo_{90-88}). Subordinated greenish *clinopyroxene* (generally 0.8-2 mm) of diopsidic composition is occasionally subhedral and dimensionally similar to olivine. In some samples it may be either interstitial or poikilitic (enclosing olivine crystals). A light yellowish, interstitial glass (around 3-5 % modal) is found within dunitic nodules. Glass may as well occur as pools surrounding granular olivine aggregates. In some cases olivine is strongly anhedral with lobate rims, thus indicating reaction with a liquid and subsequent reclying within a magma chamber. Olivine in veinlets is larger (0.5-2.5 mm) and shows a deep green color with composition within the cited mode (Fo_{90-88}). Olivine of both types may locally show deformation bands ("strain lamellae") and twinning as well as decompression textures that reflect a deep environment of formation (e.g. Mercier and Nicolas, 1974; Helz, 1987; Fig. 2a). Similar textures have been described by Conticelli and Peccerillo (1990) in several ultramafic xenoliths included in ultrapotassic lavas of Central Italy. Moreover, some olivines show abundant granular microinclusions of Cr-spinel (Figs. 2b and 2e) occasionally coexisting with Cr-rich phlogopite microinclusions (with Cr_2O_3 contents up to about 2.10 wt%). Locally, microinclusions of this phlogopite coexist with glass (Fig 2d). In some cases Cr-spinels are in pseudomorphic opacitic aggregates which likely replace a former cubic mineral phase, such as garnet and/or an earlier and larger Cr-spinel (Fig. 2c) or both. Similar textures and mineral associations replacing garnet have been described by Erlank *et al*. (1987; p. 227-252)

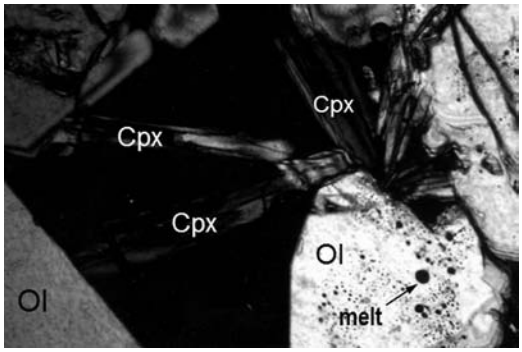

Fig. 3 – Radiating acicular late stage pyroxene (Cpx) around olivine crystals (Ol) in cumulitic dunite. This pyroxene may be associated with rare microlites of olivine (Fo_{86-85}) ± plagioclase and leucite immersed within the interstitial glass. The black area is glass (gl). Crossed polarizers. Long dimension 1.2 mm.

in garnet-phlogopite peridotites from Kimberley Pipes. Within Vesuvian dunitic nodules, olivine crystals carrying these pseudomorphic textures are in crystal clots or centimetric patches. In these domains the forsteritic olivine carrying these textures is clearer than the greenish one associated with veins.

Some specimen of dunite may show a *mosaic-equigranular texture* (Fig. 2e) typical of recrystallized mantle peridotite (e.g. Mercier and Nicolas, 1974; Helz, 1987). Porhyroclastic textures grading toward mosaic equigranular have been also found in *clinopyroxenite* nodules (Fig. 2f, sample Vs100). In these samples, elongated diopside porphyroclasts (ranging 2-4 mm) and rare anhedral porphyroclasts of olivine are surrounded by a equigranular matrix of clinopyroxene (of similar composition) and sparse opaque minerals. Clinopyroxene may show melt inclusions of tephritic composition. As previously mentioned, a second type of clinopyroxenite is represented by the outer rim of dunitic ejecta and consists of deep green *olivine bearing clinopyroxenite* (such as sample Vu65) that shows a orthocumulate heterogranular texture with crystals of diopsidic pyroxene (2-4 mm across) and rare greenish olivine of similar size. Some light brown interstitial glass of tephritic composition has also been observed.

A late, acicular Al-richer brown-greenish *clinopyroxene* (Fig. 3, elongated radiating crystals range 0.3-0.7 mm) is locally growing around

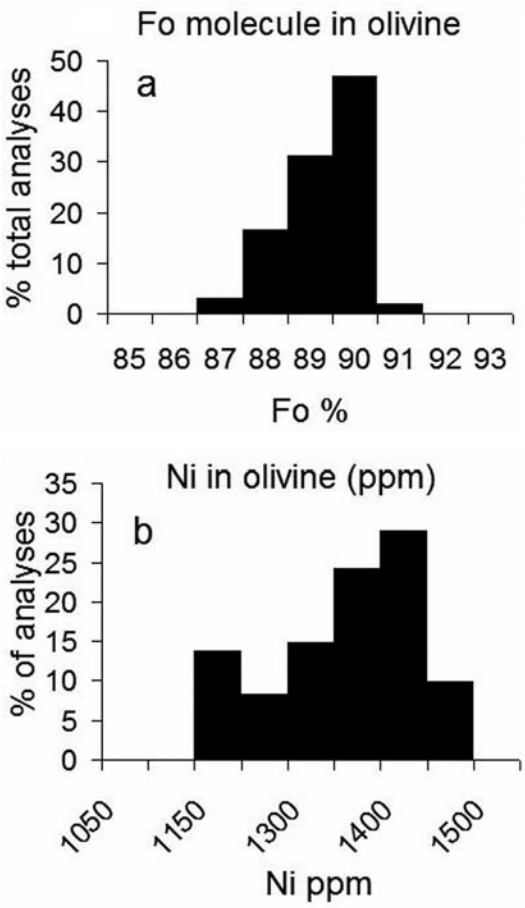

Fig. 4 – Histograms showing the average endmember compositions of olivine within the dunitic ejecta (a), and their Ni contents measured by ICP-MS Laser Ablation (b).

olivine crystals and may be associated with rare microlites of olivine (Fo_{86-85}) ± plagioclase and leucite immersed within the interstitial glass.

MINERAL AND MELT COMPOSITIONS

Mineral phases and glasses were analysed at the Department of Earth Sciences at the University of Milan by means of an ARL-SEMQ electron microprobe using natural and synthetic standards. Operating conditions were 15 keV for the accelerating voltage with a sample current of 0.015 μA. Glasses were analyzed under a 15 μm defocused beam or larger. In these cases, the acquisition time has been reduced to 30 seconds to minimize alkalis loss. Analytical one-sigma precision is estimated to be 1-2 % for major elements and 5-10 % for minor elements.

Mineral compositions

Olivine crystals of dunitic enclaves are unzoned with a composition in the range of $Fo_{90-87.5}$ with a higher frequency of Fo_{90} (Table 1, Fig. 3a). Its CaO content is generally comprised between 0.24-0.35 wt%. Lower CaO contents are in good agreement with those experimentally obtained by Adams and Bishop (1986) at high pressures. Preliminary data obtained by ICP-MS Laser Ablation at the Department of Earth Sciences of the University of Bristol (EU Geochemical Facility) indicate that these forsteritic olivines have Ni contents of 1150-1550 ppm (Fig. 4b).

Larger crystals in veins and pockets do not significantly differ in composition. Microlites of olivine of the *"quenched assemblage"* within the interstitial liquid (coexisting with clinopyroxene, plagioclase, An_{78-76}, and rarely leucite) are slightly iron richer (Fo_{86-85}) (Table 1, an. 14) and similar in composition to the olivine from Vesuvian tephritic lavas (cf. Joron *et al*., 1987).

Clinopyroxene, occurring both in large and poikilitic crystals, is unzoned and exhibits a diopsidic composition clustering at about $En_{47.5\pm2}Wo_{48\pm2}$ with variable Cr_2O_3 contents, up to 0.49-0.70 wt% (Table 2). Its Al_2O_3 content is low, ranging 0.8-1.3 in weight %. The CaTs molecule is in the range of 1-1.4 mol%. In contrast, analyzed *needles of late-stage clinopyroxene* (part of the "quenched assemblage", together with plagioclase, olivine and leucite) have higher Al_2O_3 values (up to 6.9 wt%) which increase the CaTs contents to about 8.5 mol%. This pyroxene has lower silica and slightly higher CaO and FeO contents, thus straddling toward salitic compositions $En_{39\pm2}Wo_{51\pm2}$. Similarly, the TiO_2 contents are systematically higher (Figs. 5 a, 5b). The overall chemistry of this late phase is similar to that of the lavas' phenocrystic clinopyroxene (e.g., Dolfi and Trigila, 1983; Wood and Trigila, 2000; among others).

Analyzed microinclusions of *Cr-spinel* in olivine of dunites are Cr-hercynite and chromitic spinels

TABLE 1

Representative electron microprobe analyses of olivine in dunitic cumulitic ejecta of Mount Vesuvius. Abbreviations N: regular size, LC: large crystals, qnc: quenched microlite.

Sample	Vu63	Vu65	Vu69	Vu66	Vu63	Vu63	Vu69	Vu66	Vu66	Vs83	Vs83	Vs114	Vs114	Vs108
size	N	N	N	N	LC	LC	LC	LC	LC	LC	N	LC	N	qnc
an. #	1	2	3	4	5	6	7	8	9	10	11	12	13	14
SiO_2	41.6	41.5	42.0	40.8	41.1	41.9	40.6	41.1	41.8	40.8	42.1	41.1	42.3	39.8
FeO*	10.6	9.94	9.82	10.3	11.4	9.01	11.1	11.4	10.3	12.1	10.9	12.3	10.9	14.7
MnO	0.18	0.3	0.24	0.33	-	-	0.36	0.36	-	0.21	0.22	0.23	0.18	-
MgO	47.9	47.8	48.3	48	47.6	48.7	47.6	47.6	47.9	46.8	45.8	46.1	45.9	44.8
CaO	0.24	0.33	0.25	0.32	0.32	0.33	0.36	0.32	0.28	0.3	0.33	0.26	0.37	0.36
Total	100.52	99.87	100.61	99.75	100.42	99.94	100.02	100.78	100.28	100.21	99.35	99.99	99.65	99.66
Fo	88.95	89.55	89.76	89.25	88.15	90.59	88.43	88.15	89.20	87.33	88.22	86.98	87.97	84.45

Total iron as FeO*. Dashes where not detected (<2s)

having Cr_2O_3 values averaging about 27 and 44.6 wt%, respectively (Table 3). Alumina is drastically higher in the first, whereas titania contents are higher in chromite (up to 1.8 wt%) and in hercynite are essentially below 1 wt% in hercynite. The ratio Fe^{2+}/Fe^{3+} in Cr-rich spinels does not show marked variations, thus indicating that the degree of oxidation of the magma in equilibrium with these mineral phases may be sufficiently constrained. As I will later discuss, this is a key parameter for estimating the oxygen fugacity of liquid phases involved in thermobarometric calculations. When plotted on the Cr_2O_3 versus Al_2O_3/MgO diagram these spinels define a very distinct fractionation trend (Fig. 6a). It is interesting to note that high-Cr spinels plot within the field of kimberlite with some of them straddling the field of ultramafic xenoliths in kimberlite (as shown on the Cr# versus Fe^{2+}/Fe^{2+}+Mg diagram reported in Fig. 6b).

Microinclusions of *phlogopite in olivine* do not show a marked compositional variation (Table 4). They are characterized by relatively high Cr_2O_3contents (as high as 2.2 wt%). When phlogopite microinclusions are surrounded by Cr-spinel, they usually show a dramatic decrease in chromium dioxide (down to about 0.3-0.4 wt%) since Cr would preferentially enter the spinel. Phogopite has a *mg* ratio (Mg/Mg+Fe* i.e., total iron as Fe^{2+}) ranging 0.87-0.89. A plot of this parameter versus TiO_2 is given in Fig. 7a. Noticeably, low alumina phlogopites plot within the field of macrocrysts in kimberlites. Similarly, Cr_2O_3 versus TiO_2 systematics (Fig. 7b) for ultramafic peridotites indicates that most of these micas plot in the field of secondary phlogopite, being consistent with petrographic observations, namely the absence of deformation bands and disequilibrium relationships. Nevertheless, some samples fall in the field of matrix phlogopite in kimberlites. Relatively low values in Al_2O_3 are in good agreement with those experimentally obtained by Edgar *et al*. (1976; 1980) at high pressure in ultrapotassic melts of the mafurite-ugandite series. BaO contents in these phlogopites have average contents of an average of 0.54 ± 0.17 wt%, with some samples being as high as 0.9-1.3 wt%.

Melt compositions

Selected averages of electron microprobe analyses of melt inclusions (~50-100 μm, in diameter) within olivine of the dunitic ejecta are displayed in Table 5, together with those of interstitial glasses. Analyses reported in Table 5 have been normalised to 100 wt%. All glasses are *or-ne* normative liquids (ranging 27-36.3 and 5-10, respectively), and some of them also show small amounts of normative *lc* (1-3.5). When

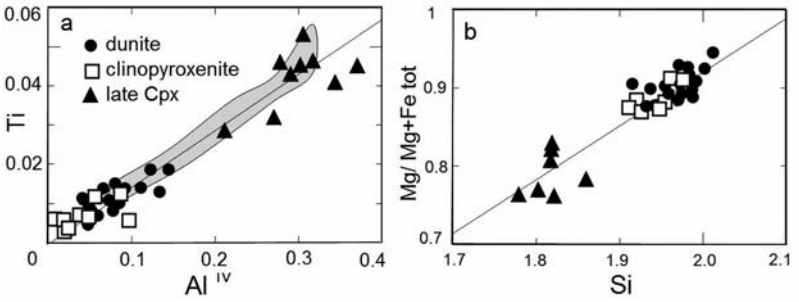

Fig. 5 – (a) Ti *vs.* Al^{IV} diagram for clinopyroxenes of the dunitic ejecta compared with those found within recent lavas. (b) Mg/

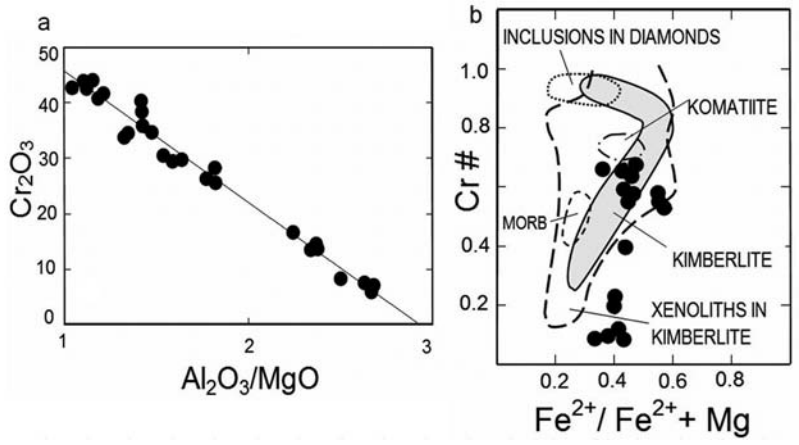

Fig. 6 – (a) Compositional variations for Cr-spinels included in forsteritic olivine of dunitic ejecta on the Cr_2O_3 *vs.* Al_2O_3/MgO diagram exhibiting a clear fractionation trend. (b) Compositional variations for Cr-spinel found as microinclusions in olivines of dunitic ejecta projected into the Cr/Al+Cr (Cr#) *vs.* Fe^{2+}/Fe^{2+}+Mg diagram. The fields for kimberlitic spinels and

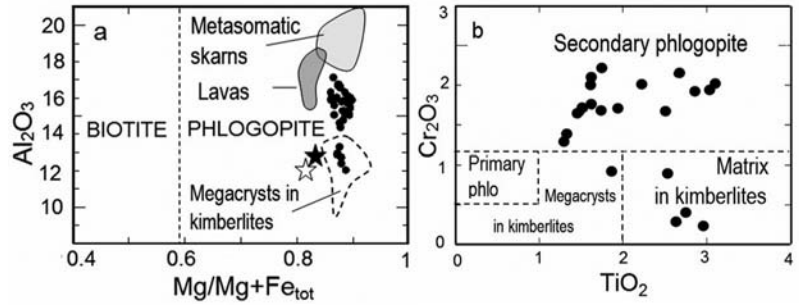

Fig. 7 – Compositional variations of phlogopite microinclusions in olivine of Vesuvian dunitic ejecta. In the Al_2O_3 *vs.* Mg/Mg+FeO_{tot} diagram (a), microinclusions are compared to phlogopites found in Vesuvian lavas, together with those found in metasomatic skarns (Fulignati *et al*., 2000a) and those of megacrystic phlogopite in kimberlites (data were compiled by Mitchell, 1986; Table 6.22, p. 204). Open and full stars are experimentally crystallised micas from "ugandite" at 10 and 20 kbar, respectively (Edgar *et al*., 1980; Table 8, sample C2811). (b) Compositional variations of phlogopite microinclusions on the Cr_2O_3 *vs.* TiO_2 diagram. Fields for megacrystal phlogopite, and primary and secondary phlogopite in lherzolite are from

TABLE 2

Selected electron microprobe analyses of clinopyroxene in dunitic and clinopyroxenitic ejecta of Mount Vesuvius. LC: large crystals; poik: poikilitic; N: regular size; qnc: quenched interstitial microlites

	DUNITES								CLINOPYROXENITES			
Sample	Vu69	Vu63	Vu67	Vu69	Vu63	Vs83	Vu69	Vs114	Vs 100	Vs 100	Vs 100	Vu65
type	LC	LC	LC	poik	poik	N	qnc	qnc	LC core	LC rim	matrix	LC
an. #	1	2	3	4	5	6	7	8	9	10	11	12
SiO_2	54.60	55.20	54.80	54.60	54.60	53.90	49.50	48.50	54.5	52.8	53.9	53.9
TiO_2	0.38	0.18	0.34	0.39	-	0.28	1.65	1.89	0.24	0.55	0.38	0.28
Al_2O_3	0.95	1.10	1.20	0.91	0.99	1.87	6.43	6.99	1.39	2.74	1.75	1.87
Cr_2O_3	0.61	0.49	0.00	0.63	0.59	0.24	-	-	0.2	-	0.21	0.24
FeO	2.51	1.92	2.57	2.48	2.53	3.73	5.36	6.52	3.3	3.82	3.43	3.73
MnO	-	0.27	-	-	-	-	-	0.22	-	-	-	-
MgO	18.30	18.20	17.70	18.35	18.20	15.50	14.30	11.80	15.7	15.2	15.9	15.5
CaO	23.10	22.20	22.90	23.18	23.10	23.90	23.10	23.40	24.4	24.3	23.9	23.9
Na_2O	-	-	-	-	-	0.60	-	0.58		0.2	-	0.24
Total	100.45	99.56	99.51	100.54	100.01	100.02	100.34	99.90	99.73	99.41	99.47	99.42

Total iron as FeO*. Dashes where not detected (<2σ)

TABLE 3

Selected electron microprobe analyses of Cr-spinels in dunitic ejecta of Mount Vesuvius.

Sample	Vs63	Vu67	Vu67	Vu63*	Vu66	Vu66	Vs83	Vs83	Vs107	Vs114
an. #	1	2	3	4	5	6	7	8	9	10
SiO_2	-	-	-	-	-	-	-	-	0.2	-
TiO_2	1.62	1.62	1.07	1.41	0.63	0.87	1.2	0.72	1.43	0.95
Al_2O_3	14.9	14.92	15.71	19.44	27.9	27.5	40.6	50.1	16.7	46.25
Cr_2O_3	43.7	43.69	43.57	37.60	28.2	27.7	13.6	6.64	34.6	7.04
Fe_2O_3	11.56	10.78	11.89	13.20	14.98	14.96	14.88	12.92	16.61	15.55
FeO*	15.39	15.1	14.84	13.97	13.62	13.64	13.21	11.13	17.66	13.01
MnO	-	-	-	-	-	0.22	-	0	0.32	0.25
MgO	13.4	13.37	13.52	14.58	15.2	15.1	17.1	18.9	11.3	17.59
CaO	-	-	-	-	0.12	-	0.17	0	-	-
Total	100.57	99.48	100.6	100.20	100.65	99.99	100.76	100.4	99.37	100.64
mg	48.07	49	48.54	50.13	49.99	49.82	53.39	59.68	38.18	53.72
Fe^{2+}/Fe^{3+}	1.480	1.557	1.387	1.176	1.010	1.013	0.987	0.957	1.182	0.930

Fe3+ calculated according to the stoichiometry. Dashes where not detected (<2σ)

TABLE 4
Selected electron microprobe analyses of phlogopite microinclusions in olivine of dunitic ejecta of Mount Vesuvius

Sample	Vu63	Vu67	Vu69	Vu69i/S1	Vu69	Vu69 core	Vu69 rim	Vu69cS core	Vu69rS3 rim	Vu69cS1 core	Vu69rS1 rim
an. #	1	2	3	4	5	6	7	8	9	10	11
SiO_2	39	38.5	37.4	39.1	37.5	37.4	37.5	38.8	39	38.2	39.0
TiO_2	1.52	1.54	2.98	1.31	3.02	3.03	2.86	1.86	2.46	1.32	1.77
Al_2O_3	16.1	16.3	15.2	12.7	15.1	15.3	15.1	12.8	15.6	12.04	16.1
Cr_2O_3	1.68	1.7	1.93	1.28	1.96	1.95	1.93	0.9	1.63	1.38	1.72
Fe_2O_3	0.09	0.09	0.15	0.16	0.16	0.14	0.16	0.15	0.12	0.19	0.14
FeO	5.77	5.84	4.78	6.35	4.71	4.98	4.95	6.79	5.65	6.28	4.82
MgO	20.2	20.5	22.5	26.7	22.7	21.9	22.9	26.6	21.8	28.6	22
CaO	0.17	-	-	-	-	-	-	0.96	-	-	-
Na_2O	0.43	0.43	0.17	0.43	0.16	0.16	0.19	-	-	0.94	-
K_2O	9.41	9.52	9.82	7.67	9.8	9.81	10.3	7.14	9.29	7.1	9.94
BaO	0.61	0.63	0.81	0	0.85	0.83	0.84	-	-	-	-
Cl	0.05	0.05	0.02	0	0.02	0.02	0.08	-	-	-	-
F	0.43	0.44	0.47	0	0.59	0.1	0.55	-	-	-	-
H_2O	3.64	3.66	3.68	3.84	3.73	3.81	3.64	3.96	3.99	3.81	3.84
Total	99.1	99.2	99.91	99.54	100.3	99.43	101	99.96	99.54	99.86	99.33

Fe_2O_3 and water calculated at 1 bar and 1100°C along the Ni-NiO buffer, according to Righter and Carmichael (1996).
Dashes: not detected (<2σ)

plotted on the TAS diagram of Le Bas (1986), most of the glasses of melt inclusions plot within the phono-tephrite field straddling the trachybasalt field and the tephrite-basanite field (Fig. 8). Few show trachybasaltic, and basaltic compositions. Interstitial glasses are slightly more evolved and are essentially of phono-tephritic composition. It is significant to point out that the trend defined by these glasses overlap the fractionation trend of Vesuvian lavas which is characterised by an increase of alkali together with a decrease in MgO and FeO for relatively constant SiO_2 contents (cf. Trigila and De Benedetti, 1993). Both glasses (in melt inclusions and interstitial) have a relatively high P_2O_5 contents, typical feature of the Vesuvian lavas and tephra (cf., Joron *et al*., 1987). *Primitive melts*, found as brownish microinclusions within the olivine, are basalt and trachybasalt (Table 5). Their Mg# values (defined as 100 Mg/Mg+Fe*, i.e. total iron as Fe^{2+}) are up to 71-75. These are minimum values since all iron was assumed to be ferrous. Alumina contents are lower (14.2-14.8 wt%, Table 5, an. 2 and 3) when compared to more evolved melts.

Roeder and Emslie (1970) suggested a value of 0.33 for the Fe-Mg distribution coefficient between olivine and melt ($K_D^{Ol\text{-}liq}$). Therefore, an olivine of forsteritic composition (~Fo_{90}) would be equilibrium with a melt of Mg# ~ 75. According to Kamesky *et al*. (1999), if olivine is crystallising with clinopyroxene the above distribution coefficient would decrease to 0.27, and the Mg# of

TABLE 5

Representative selected melt compositions (normalised to 100 wt%) in dunitic ejecta from Mount Vesuvius. See text for details. Abbreviations, in: microinclusion; in+phlo: microinclusions of phlogopite coexisting with glass.

	MELT INCLUSIONS						INTERSTISTIAL GLASS				
Sample	Vu63-tb	Vu63-in/b	Vu63-in/g	Vu69	Vu69	VS 83 in	Vu63 int	Vu67int	Vu69	Vs114 int	VS83-int
rock	dun	dun	dun	dun	dun	dun	dun	dun	dun	dun	dun
type	in	in	in	in+phlo	in+phlo	in	int	int	int	int	int
an #	1	2	3	4	5	6	7	8	9	10	11
SiO_2	49.73	51.15	50.22	50.64	55.43	50.07	50.23	49.68	50.65	50.19	50.44
TiO_2	0.57	0.80	0.73	0.80	1.17	0.88	1.11	1.08	1.12	0.84	1.10
Al_2O_3	14.81	14.16	14.45	15.91	17.75	15.38	15.93	18.28	16.03	17.34	15.75
Cr_2O_3	0.19	0.21	0.21	0.04	0.00	0.02	0.02	0.04	0.04	n.d	0.04
FeO*	6.76	5.78	6.01	5.77	5.20	6.97	6.48	6.75	7.03	7.55	6.43
MnO	n.d.	0.16	0.17	0.12	n.d	0.11	0.25	0.20	n.d	0.16	0.26
MgO	9.54	8.63	10.01	6.82	1.19	4.34	5.62	4.40	4.51	3.55	4.40
CaO	9.93	10.99	10.27	10.75	13.39	13.87	11.43	12.09	12.25	9.91	12.45
Na_2O	1.81	1.59	1.60	2.19	1.25	1.76	2.28	1.97	1.96	2.56	2.12
K_2O	5.35	5.31	4.98	5.68	3.53	5.07	5.38	4.32	5.15	6.50	5.72
P_2O5	0.89	0.97	0.95	0.94	0.75	1.06	0.91	0.85	0.89	0.90	0.89
BaO	0.41	0.24	0.40	0.34	0.33	0.46	0.37	0.34	0.36	0.51	0.40
Mg#	71.54	72.69	74.8	67.82	29.03	52.63	60.68	53.75	53.37	45.58	54.9
Fo host	89.2	89	89.5	89.2	88.5	87.7					

* Total iron as FeO*. n.d.: not detected.

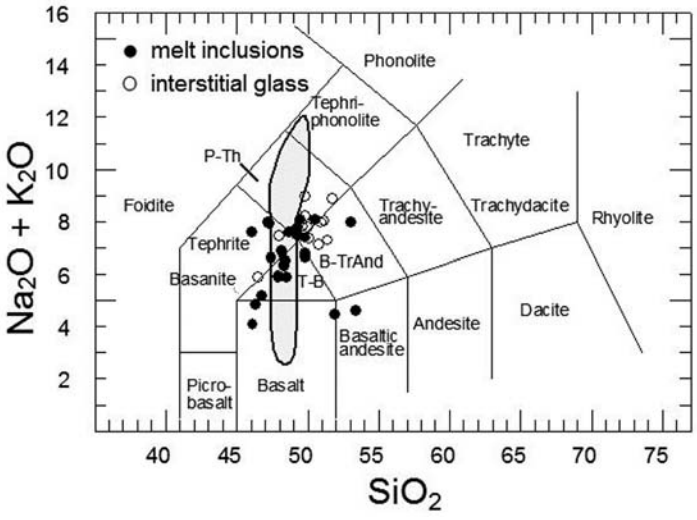

Fig. 8 – Melt inclusions in forsteritic olivine and interstitial glasses plotted on the TAS diagram of Le Bas *et al*. (1986). The field delimited by the heavy line is the distribution of Vesuvius historical lavas (after Trigila and De Benedetti, 1993).

the coexisting melt will be nearly 71. Therefore, the average melt composition used in thermodynamic calculations (involving analyses 1, 2 and 3 of Table 5) have not been adjusted since minor variations in melt chemistry will result in negligible changes of P-T estimates. Glasses coexisting with Cr-rich phogopite are slightly more evolved with a Mg# around 65 (Tab. 5, analyses 6 and 7). In some cases glasses coexisting with phlogopite are completely depleted in MgO, FeO and, to a lesser extent, Al_2O_3, indicating post-trapping crystallisation of olivine ± phlogopite (for additional data see also Cigolini, 1997).

Interstitial light-brownish glasses show a broader compositional variation with lower Mg#, ranging 46-61, and higher contents in alkalis (with K_2O ranging 4.2-6.5 wt%).

Melt inclusions were recently investigated by FTIr spectrometry and show H_2O contents ranging from 1.15 to 2.4 wt%, and CO_2 comprised between 0.1 and 0.21 wt% (Laiolo, 2004). Interstitial melts are degassed with lower H_2O (up to ~0.45 wt%) and CO_2 contents (up to 0.02 wt%).

THERMOBAROMETRY

The lack of orthopyroxene in this ultramafic cumulates precludes the use of the two-pyroxene geothermometer of Köler and Brey (1990). Similarly, the presence of phlogopite rules out the application of Loucks' geothermometer (Loucks, 1996) for the coexisting olivine and clinopyroxene since is strictly applicable to nearly anhydrous assemblages. However, I have used equation (2) of Köler and Brey (1990) to have an indirect estimate of temperature (i.e., $T \geq 1100°C$) since their equation (3) is never satisfied by the data. The use of the computer code QUILF (Andersen *et al*., 1993) for the coexisting olivine-clinopyroxene-melt assemblage gave temperatures ranging 1250-1320°C (Cigolini, 1997). The use of Mercier's clinopyroxene thermobarometer (Mercier, 1980) gives discordant temperatures, ranging 920-1050°C and excessively high pressure regimes for some samples (comprised between 33 and 13 kbar, neglecting quenched crystals in the mesostasis). Kretz's geothermometer (Kretz, 1982) gives discordant temperatures as well (ranging, 870-1295°C).

The Righter and Charmichael's geothermometer (Righter and Charmichael, 1996), based on the partitioning of TiO_2 between phlogopite and the coexisting silicate liquid, gives temperatures of 1000-1150°C. Similarly, estimated temperatures for the coexistence of olivine with Cr-spinel (Roeder *et al*., 1979) yield values of 1040-1180°C. Noticeably, lower temperatures are related to thermal re-equilibration at depth (cf., Frost and Lindsley, 1991), thus implying that the ultramafic assemblage underwent significant cooling before being included in the uprising tephritic magmas that finally brought them up to the surface.

In order to have a better constrain on the P-T regimes associated with solid-melt equilibrium relationships, I constructed a grid of reactions (Fig. 8) that would adequately describe our system. These are the following:

$$Mg_2SiO_4 = Mg_2SiO_4 \quad (1)$$
Fo (sol) = Fo (liq)

$$Mg_2SiO_4 + SiO_2 = Mg_2Si_2O_6 \quad (2)$$
Fo (sol) liq CEn

$$(CaMg)Si_2O_6 = \tfrac{1}{2}\,SiO_2 + \tfrac{1}{2}\,Mg_2SiO_4 + CaSiO_3 \quad (3)$$
Di liq Fo (sol) Wo (liq)

$$CaAl_2Si_2O_8 + 2Mg_2SiO_4 + SiO_2 = 2Mg_2Si_2O_6 + CaAl_2SiO_6 \quad (4)$$
An Fo (sol) liq CEn CaTs

The above heterogeneous equilibria treat melts components in equilibrium with the coexisting solid phases. Reactions (1) to (3) have been used to assess equilibrium conditions for the high pressure (HP) assemblage by considering olivine and clinopyroxene in equilibrium with the primitive melts found as microinclusions in olivine (the average composition of analyses 1, 2 and 3 reported in Table 5 has been used in calculations). In this case, I have assumed that equilibrium conditions occur along the olivine-clinopyroxene cotectic, as postulated by Kelemen (1990) for basaltic melts interacting with peridotitic materials.

Equilibrium conditions for the low pressure (LP) assemblage have been determined on the basis of reaction (1), (3) and (4). This assemblage is represented by the *"quenched"* acicular clinopyroxene coexisting with minute

TABLE 6

Summary of thermodynamic solutions for reactions (2) and (3). The melt composition is given by the average of trachybasaltic melts inclusions reported in Table 5 (analysis 1, 2 and 3). Activities of clinoenstatite and diopside molecules in clinopyroxene has been calculated according to Gasparik (1990) for analysis 1, Table 2. Activities for olivine are calculated according to Sack and Ghiorso (1989). See text and Fig. 9a.

Reaction (2): $Mg_2SiO_4 + SiO_2 = Mg_2Si_2O_6$

T °C	P (kbar)	$\Delta G_0^{1,T}$	H_2O %	a_{Fo} (sol)	a_{CEn}	$Loga_{SiO2}$
1000	11.05	-6.230	3.5	0.830	0.799	-0.570
1100	12.16	-5.014	3.5	0.827	0.693	-0.570
1200	13.50	-3.674	3.5	0.825	0.613	-0.569
1300	15.03	-2.215	3.5	0.822	0.550	-0.568
1400	16.76	-0.642	3.5	0.821	0.500	-0.568
1000	10.31	-6.230	2.5	0.830	0.799	-0.554
1100	11.27	-5.014	2.5	0.827	0.693	-0.551
1200	12.43	-3.674	2.5	0.825	0.613	-0.549
1300	13.80	-2.215	2.5	0.822	0.550	-0.546
1400	15.36	-0.642	2.5	0.821	0.500	-0.544
1000	9.43	-6.230	1.5	0.830	0.799	-0.533
1100	10.22	-5.014	1.5	0.827	0.693	-0.529
1200	11.22	-3.674	1.5	0.825	0.613	-0.525
1300	12.42	-2.215	1.5	0.822	0.550	-0.521
1400	13.81	-0.642	1.5	0.821	0.500	-0.518

Reaction (3): $(CaMg)Si_2O_6 = ½\ SiO_2 + ½\ Mg_2SiO_4 + CaSiO_3$

T °C	P (kbar)	$\Delta G_0^{1,T}$	H_2O %	a_{Fo} (sol)	a_{Di}	a_{Wo} (liq)	$Loga_{SiO2}$
991	0.001	30.861	3.5	0.830	0.884	0.099	-0.569
1200	10.65	25.318	3.5	0.825	0.881	0.101	-0.569
1300	17.63	22.172	3.5	0.822	0.879	0.102	-0.568
1400	26.59	18.741	3.5	0.821	0.878	0.103	-0.568
1500	38.37	15.047	3.5	0.819	0.877	0.104	-0.568
1014	0.001	30.314	2.5	0.829	0.883	0.108	-0.552
1200	9.19	25.318	2.5	0.825	0.881	0.110	-0.548
1300	15.80	22.172	2.5	0.822	0.879	0.111	-0.547
1400	24.26	18.741	2.5	0.821	0.878	0.112	-0.545
1500	35.42	15.047	2.5	0.819	0.877	0.113	-0.544
1043	0.001	29.621	1.5	0.829	0.883	0.119	-0.530
1200	7.54	25.318	1.5	0.825	0.881	0.121	-0.524
1300	13.77	22.172	1.5	0.822	0.879	0.123	-0.521
1400	21.67	18.741	1.5	0.821	0.878	0.124	-0.518
1500	32.12	15.047	1.5	0.819	0.877	0.125	-0.516

$\Delta G_0^{1,T}$ (kJ)

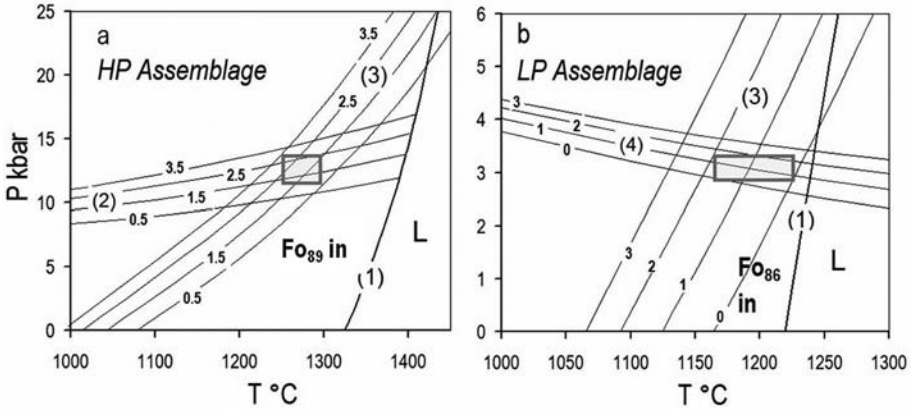

Fig. 9 – Thermodynamic solutions for selected heterogeneous equilibria involving primitive melts and "coexisting" mineral phases under variable hydrous conditions. (a) Equilibrium conditions for the high pressure assemblage represented by olivine (Fo_{89}) clinopyroxene coexisting with a trachybasaltic melt. The graph summarizes the P-T grid obtained by solving thermodynamically reactions (1), (2), (3) indicated by the large numbers in parentheses. Smaller numbers are the water contents within the melt (wt% H_2O). Best solutions are outlined by the rectangle (see text). (b) Equilibrium conditions for the low pressure assemblage ("quenched assemblage") consisting of secondary olivine (Fo_{86}), clinopyroxene and plagioclase (An_{78}) coexisting with a trachybasaltic melt. The graph summarizes the P-T grid obtained by solving thermodynamically reactions (1), (2), and (4) indicated by the large numbers in parentheses. Smaller numbers are the water contents within the melt (wt% H_2O). Best solutions are outlined by the rectangle (see text).

plagioclase (An_{78-76}) and a slightly more iron rich olivine (Fo_{86-85}) that nucleates within the interstitial melt. Activities where calculated for the interstitial melt reported in Table 5 (analysis 7) and for the late acicular pyroxene (analysis 7, Table 2).

Gibbs free energies and volume expansion and compressibilities have been calculated using the thermodynamic data of Berman (1988; Table 2 and 3, and Table 4 for volumes, p. 458-463) on ferromagnesian phases, together with those of Richet *et al*. (1982) for amorphous silica, and those of Ghiorso and Sack (1995) for other melt components (a synopsis of the latter data is given by Ghiorso and Sack, 1995; Table A1, p. 209). A summary of thermodynamic data used in calculation is given in the Appendix (Table A1).

Activity models used in calculations are the following: olivine, Sack and Ghiorso (1989); clinopyroxene, Gasparik (1984; 1990); plagioclase, Newton *et al*. (1980). Activities for liquid components have been calculated according to Ghiorso and Sack (1995).

The degree of oxidation of the system has been retrieved using the relationship of Marianelli *et al*. (1995) that relates the cation ratio Fe^{2+}/Fe^{3+} in Cr-spinels with the oxygen fugacity of the melt. If a ratio of 1.5 (i.e., the ratio obtained in high Cr-spinels) is used for spinels in equilibrium with a trachybasaltic melt, I obtain (by introducing the algorithm of Kress and Carmichael, 1991) oxygen fugacities within 0.5 log units of Ni-NiO buffer of Hübner and Sato (1970). By using a ferrous/ferric cation ratio of 1, oxygen fugacities would be within 2 log units above the cited buffer. Therefore, I used this buffer in estimating fugacities within the melt by systematically applying the algorithm of Kress and Carmichael (1991), and taking into account the effect of pressure on the Ni-NiO buffer itself (in the light of the data of Robie *et al*., 1978). For reference, the numerical solutions for high-pressure assemblage given by reactions (2) and (3) are reported in Table 6.

Fig. 9a shows that equilibrium conditions for the *trachybasaltic melt* (Table 5, average of analyses 1, 2 and 3) coexisting with olivine (Fo_{89}) and clinopyroxene (analysis 1, Table 2) under hydrous conditions is rather well constrained by the curves relative to reactions (1), (2) and (3). Their intersections give an equilibration pressures of 12.4-13 kbar for temperatures of

1250-1290°C and water contents ranging from 1.5 to 2.5 wt% (which are consistent with the previously cited FTIr measurements). These results are in good agreement with previous preliminary thermobarometric estimates: 12-14 ± 2.6 kbar pressure and temperatures of 1286 ± 40°C (cf., Cigolini, 1997).

In turn, more evolved tephritic melts equilibrate with the LP "quenched" assemblage at lower pressures and temperatures (3.3-3 kbar and 1220-1170°C, respectively) before being erupted under nearly anhydrous conditions (Fig. 9b). These regimes are consistent with the storage of the cumulitic materials within a magma reservoir located in the subvolcanic region. In particular, equilibration temperatures are basically in agreement with lava effusion temperatures recorded at Vesuvius (Scandone and Giacomelli, 1998).

An open question is whether the magma was already hydrated at high pressure or inherited its water content at lower pressures. It seems likely that ascending magmas, following interaction with wall-rock and deep-seated cumulitic materials, have undegone extensive crystallization probably associated with hydration. Geothermometric data on microinclusions of Cr-rich phlogopites indicate maximum equilibration temperatures of 1150°C (the uncertainty of Righter and Carmichael geothermometer being ± 50°C) and are consistent with this scenario. However, fractionation of secondary phlogopite would, in turn, contribute to buffer the water content of the magma so that it could decrease substantially during magma ascent and storage.

Discussion and conclusions

This work has been focussed in providing new mineral chemistry data and thermobarometric estimates on some peculiar ultramafic ejecta preserved as xenoliths in 1906 pyroclastic deposits of Mount Vesuvius. These xenoliths are essentially clinopyroxene-bearing dunites and clinopyroxenites and carry textural features typical of mantle peridotite. Some of them have been tectonized and exhibit mosaic-equigranular and porphyroclastic textures. Moreover, some olivine crystals in dunite show melt inclusions of trachybasaltic composions as well as more differentiated melts of tephritic to phonotephritic composition which may coexist with Cr-rich phlogopite.

Dunites are interpreted as deep cumulates that were formed during percolation from the upper mantle (e.g., Godard *et al*., 1995) and/or storage at depth of Vesuvian-type basalts and were transported at upper crustal level by ascending magmas. Thermobarometric estimates performed by means of a grid of selected reactions indicate that these dunitic materials equilibrated with primitive trachybasaltic melts in proximity and/or below the crust-mantle transition, located at a depth of 30-36 km below Mount Vesuvius (Ferrucci *et al.*, 1989; Pontevivo and Panza, 2006). Extensive fractionation is likely to occur within this region. Ponding of basic magma at the base of the crust has been first suggested by Hildreth (1981) and Herzberg *et al*. (1983). Its ascent may be neutralised by the filtering action of the overlaying crustal rocks and solid-melt interactions may take place together with recycling of cumulitic materials (Kelemen, 1990). Ultramafic "recycled" nodules may thus contain "disaggregated portions" of the mantle wedge that may bear relict psuedomorphic textures of opacitic aggregates consisting of Cr-spinels likely replacing a former cubic mineral phase such as garnet and/or an earlier and larger spinel. By reaction with these heterogeneous deep seated cumulitic materials, the primitive melts will evolve, undergoing decompression, into tephritic melts. In turn, these differentiated melts will react with the ultramafic nodules and equilibrate at about 3 kbar and 1220-1170°C. These regimes are consistent with the existence of a sector of an upper reservoir (located at 9-10 km depth) where deep cumulitic materials are passively carried, and are momentarily stored together with tephritic magmas, before being erupted during paroxysmal eruptions. This is in good agreement with recent geophysical data, obtained by high-resolution seismic tomography (Zollo *et al*., 1998), that indicate the existence of a very low-velocity zone

at a depth of about 10-12 km below Mount Vesuvius. This discontinuity is likely to represent the "top" of an extended magma chamber which seems to have a nearly horizontal sill-like structure (Auger *et al*., 2001; Di Renzo *et al*., 2007).

On petrogenetic grounds, the presence of primitive melt inclusions of trachybasaltic compositions , together with the occurrence of Cr-rich "secondary phlogopite" support the idea that Vesuviam magmas were formed in a metasomatised mantle source (e.g. Peccerillo, 1999; Schiano et *al*., 2004; among others) likely enriched in "primary phlogopite". Primitive melts experienced extensive fractionation of olivine and clinopyroxene, minor spinel and "secondary phlogopite" before being stored within an upper reservoir, where they were eventually contaminated by Hercynian basement rocks and/or the Mesozoic limestone (cf. Di Renzo *et al*., 2007).

Future work should be oriented in collecting additional data on melt inclusions and ultramafic materials to better decode their petrogenesis as well as the complex dynamics of Vesuvius plumbing system.

APPENDIX

The Gibbs free energy for the listed reactions have been calculated according to

$$\Delta G_0^{P,T} = \Delta G_0^{1,T} + RT \ln K + \int_1^P \Delta V dP \quad \text{(A1)}$$

where $\Delta G_0^{1,T}$ is the the Gibbs free energy for the given reaction calculated at 1 bar and at the temperature of interest (T) by using the data of Berman (1988). R is the gas constant and K is the equilibrium constant which may be calculated (by knowing the chemical compositions of the phases considered) from the appropriate activities according to solution models (see text). The last term is the difference of the molar volumes for the given phases integrated within the reference pressure range. The above equation can be solved numerically for equilibrium conditions by minimizing the free energy $\Delta G_0^{P,T}$ (which goes to zero at equilibrium) by fixing a given value of T and calculating P (or vice versa). The thermodynamic data of Berman (1988) for minerals, together with those listed by Ghiorso and Sack (1995) for the melt components, have been used in calculations. A synopsis of these data for endmember components, solids and liquids, is given in Table A1.

Equilibrium constants for the reactions considered were calculated as following (subscripts for K refer to reaction numbers reported in the text):

$$K_1 = a_{Fo}^{liq} / a_{Fo}^{sol}$$

$$K_2 = a_{CEn} / a_{Fo}^{liq} a_{SiO_2}^{liq}$$

$$K_3 = (a_{SiO_2}^{liq})^{1/2} (a_{Fo}^{liq})^{1/2} a_{Wo}^{liq} / a_{Di}$$

$$K_4 = (a_{CEn})^2 a_{CaTs} / a_{An} (a_{Fo}^{sol})^2 a_{SiO_2}^{liq}$$

ACKNOWLEDGEMENTS

This work is dedicated to E. Callegari for his valued advice throughout the years and his commitment and enthusiasm in promoting Volcanology at the University of Torino. The project was funded by the Italian Ministry for Universities and Research (MURST) and by INGV. Part of the analytical work has been carried on at the "Large Scale Geochemical Facility", operative at the Department of Earth Sciences of the University of Bristol (U.K.) under the financial support of the European Commission. P. Fumagalli and R. Vannucci provided reviews of an earlier draft of the paper. Eugene Jarosewich, of the Smithsonian Institutions, provided standard glass samples.

TABLE A1

Selected thermodynamic properties of endmember solids and liquids used in calculations. Data for solids are from Berman (1988), data for liquids are from Ghiorso and Sack (1995, and references therein)

Phase	Formula	ΔH_f^0 J	ΔS_f^0 J /°K	$\overline{V^0}$ J/bar	heat capacity coefficients k_0	$k_1 \times 10^{-2}$	$k_2 \times 10^{-5}$	$k_3 \times 10^{-7}$	volume coefficients $v_1 \times 10^6$	$v_2 \times 10^{12}$	$v_3 \times 10^6$	$v_4 \times 10^{10}$
Anorthite	$CaAl_2Si_2O_8$	-4228730	200.19	10.08	439.37	-37.34	0.00	-31.702	-1.272	3.176	10.918	41.985
Ca-Tschermak	$CaAl_2SiO_6$	-3298767	140.75	6.356	310.7	-16.72	-74.553	94.878	-0.870	2.171	22.250	52.863
Clinoenstatite	Mg_2SiO_6	-3091852	132.65	6.266	279.92	-9.94	-88.004	107.142	-1.498	0.894	49.312	149.34
Forsterite	Mg_2SiO_4	-2174420	94.01	4.366	238.64	-20.01	0.00	-11.624	-0.791	1.351	29.464	88.633
Diopside	$(CaMg)Si_2O_6$	-3200583	142.5	6.62	305.41	-16.05	-71.66	92.184	-0.872	1.707	27.795	83.082
Pseudowoll.	$CaSiO_3$	-1627427	85.279	4.016	141.16	-4.172	-58.576	94.074	-1.245	3.113	28.18	0.00

Melt component	Reference solid	T_f	ΔS_f^0 J / °K	ΔC_p^0 J / °K	$\overline{V^0}$ J/bar 1673 °K	$\left(\frac{\partial \overline{V^0}}{\partial T}\right)_P \times 10^4$	$\left(\frac{\partial \overline{V^0}}{\partial P}\right)_T \times 10^5$	$\left(\frac{\partial^2 \overline{V^0}}{\partial P \partial T}\right)_T \times 10^8$	$\left(\frac{\partial^2 \overline{V^0}}{\partial P^2}\right) \times 10^{10}$
SiO_2 *	Amorph. silica	1999	4.46	81.37	2.69	0.00	-1.89	1.30	3.60
Mg_2SiO_4	Forsterite	2163	57.2	271	4.98	5.24	-1.35	-1.30	4.10
$CaSiO_3$	Pseudowoll.	1817	31.5	172.4	4.347	2.92	-1.55	-1.60	3.90

* For amorphous silica below 1480 °K: $\Delta H_f^0 = 901554$; $\Delta S_f^0 = 48.475$; $\Delta C_p^0 = 127.3 - 10.777 \cdot 10^{-3} T + 4.3127 \cdot 10^5 / T^2 - 1463.8 / \sqrt{T}$
(cf. Richet *et al.*, 1982).

REFERENCES

ANDERSEN D.J., LINDSLEY D.H.and DAVIDSON P.M. (1993) − *QUILF: a Pascal program to assess equilibria among Fe-Mg-Mn-Ti oxides, pyroxenes, olivine, and quartz*. Comp. Geosci., **19**, 1333-1350.

AUGER A., GASPARINI P., VIRIEUX J. and ZOLLO A. (2001) − *Seismic evidence of an extended magmatic sill under Mt.Vesuvius.* Science, **294**, 1510-1512

BARBERI F., and LEONI L. (1980) − *Metamorphic carbonate ejecta from Vesuvius Plinian eruptions: evidence for the occurrence of shallow magma chambers.* Bull. Volcanol., **43**, 107-120.

BELKIN H.E., DE VIVO B., ROEDDER E. and CORTINI M. (1985) − *Fluid inclusion geobarometry from ejected Mt. Somma-Vesuvius nodules*. Am. Mineral., **70**, 288-303.

BELKIN H.E., and DE VIVO, B. (1993) − *Fluid inclusion studies of ejected nodules from plinian eruptions of Mt. Somma-Vesuvius*. J. Volcanol. Geotherm. Res., **58**, 89-100.

BELKIN H.E., DE VIVO B., TÖRÖK K. and WEBSTER, J.D. (1998) − *Pre-eruptive volatile content, melt-inclusion chemistry, and microthermometry of interplinian Vesuvius lavas (pre-A.D. 1631)*. J. Volcanol. Geotherm. Res., **82**, 79-95.

BERMAN R.G. (1988) − *Internally consistent thermodynamic data for stoichiometric minerals in the system* Na_2O-K_2O-CaO-MgO-FeO-Fe_2O_3-Al_2O_3-SiO_2-TiO_2-H_2O-CO_2. J. Petrol., **29**, 445-522.

CIGOLINI C. (1997) − *Thermobarometry of phlogopite-bearing dunitic enclaves from Mount Vesuvius: preliminary estimates.* Atti Accad. Sci. Torino, Cl. Sci. Fis. Mat. Nat., **131**, 33-56.

CIGOLINI C. (1999) − "High pressure" dunitic ejecta of kimberlitic affinity in recent pyroclastic deposits from Mount Vesuvius: inference on their genesis and evolution. Atti Accad. Sci. Torino, Cl. Sci. Fis. Mat. Nat., **133**, 1-10.

CIONI R., CIVETTA L., MARIANELLI P., METRICH N., SANTACROCE R. and SBRANA, A. (1995) − *Compositional layering and Syneruptive mixing of a Periodically Refilled Magma Chamber: the AD 79 Plinian eruption of Vesuvius*. J. Petrol., **36-3**, 739-776.

CONTICELLI S. and PECCERILLO A. (1990) − *Petrological significance of high pressure ultramafic xenoliths from ultrapotassic rocks of Central Italy*. Lithos, **24**, 305-322.

CORTINI M., LIMA A. and DE VIVO B. (1985) − *Trapping temperatures of melt inclusions from ejected Vesuvian mafic xenoliths.* J. Volcanol. Geotherm. Res., **26**, 167-172.

CUNDARI A. (1982) − *Petrology of clinopyroxenite Ejecta from Somma-Vesuvius and their genetic implications*: Tscherm. Min. Petr. Mitt., **30**, 17-35.

DI RENZO V., DI VITO M.A., ARIENZO I., CARAMENTE A., CIVETTA L., D'ANTONIO M., GIORDANO F., ORSI G. and TONARINI S. (2007) − *Magmatic History of Somma-Vesuvius on the Basis of New Geochemical and Isotopic Data from a Deep Borehole (Camaldoli dellaTorre)*. J. Petrol., **48/4**, 753-784

DOLFI D. and TRIGILA R. (1983) − *Clinopyroxene solid solutions and water in magmas: results in the system phonolitic tephrite-*H_2O. Mineral. Mag., **47**, 347-351.

EDGAR A.D , GREEN D.H. and HIBBERSON W.O. (1976) − *Experimental petrology of a highly potassic magma*. J. Petrol., **17**, 339-356.

EDGAR A.D., CONDLIFFE E., BARNETT R.L. and SHIRRAN R.J. (1980) − *An experimental study of an olivine ugandite magma and mechanics for the formation of its K-enriched derivatives*. J. Petrol., **21**, 475-497.

ERLANK A.J., WATERS F.G., HAWKESWORTH C.J., HAGGERTY S.E., ALLSOPP H.L., RICKARD R.S. and MENZIES M.A. (1987) − *Evidence for Mantle Metasomatism in Peridotite Nodules from Kimberley Pipes, South Africa.* In: Menzies M.A. and Hawkesworth C.J. (Eds.), Mantle Metasomatism. Academic Press, London, 221-311.

FERRUCCI F., GAUDIOSI G., PINO N.A., LUONGO G., HIRN A. and MIRABILE N. (1989) − *Seismic detection of a major Moho upheaval beneath the Campania volcanic area (Naples, Southern Italy)*. Geophys. Res. Lett., **16**, 1317-1320.

FROST B.R. and LINDSLEY D.H. (1991) − *Occurrence of Iron-Titanium Oxides in Igneous Rocks.* In: Lindsley D.H. (Ed.), Oxide Minerals: Petrologic and Magnetic significance. MSA Rev. Mineral., **25**, 433-468.

FULIGNATI P., MARIANELLI P. and SBRANA A. (2000a) − *The skarn shell of the 1944 Vesuvius magma chamber, Genesis and P-T-X conditions from melt and fluid inclusions*. Eur. J. Mineral., **12**, 1025-1039.

FULIGNATI P., MARIANELLI P. and SBRANA, A. (2000b) − *The feeding system of the 1944 eruption of Vesuvius: melt inclusions data from dunitic nodules.* N. Jb. Miner. Mh, **9**, 419-432.

GASPARIK T. (1984) − *Two pyroxene thermobarometry*

with new experimental data in the system CaO-MgO-Al_2O_3-SiO_2. Contrib. Mineral. Petrol., **87**, 87-97.

GASPARIK T. (1990) − *A thermodynamic model for the enstatite-diopside join*. Am. Mineral., **75**, 1080-1091.

GHIORSO M.S. and SACK R.O. (1995) − *Chemical mass transfer in magmatic processes IV. A revised and internally consistent thermodynamic model for the interpolation and extrapolation of liquid-solid equilibria in magmatic systems at elevated temperature and pressures*. Contrib. Mineral. Petrol., **119**, 197-212.

GODARD G., BODINIER J.L. and VASSEUR, G. (1995) − *Effects of mineralogical reactions on trace-element redistribution in mantle rocks during percolation process: a chromatographic approach*. Earth Planet. Sci. Letters, **133**, 449-461.

HELZ R.T. (1987) − *Diverse olivine types in lava of the 1959 eruption of Kilauea Volcano and their bearing on the eruptions dynamics.* In: Decker R.W., Wright T.L. and Stauffer P.H. (Eds.), Volcanism in Hawaii. USGS Prof. Paper n. 1350, p. 691-722.

HERMES O.D. and CORNELL W.C. (1981) − *Quenched crystal mush and associated magma compositions as indicated by intercumulus glass from Mount Vesuvius, Italy*. J. Volcanol. Geotherm. Res., **2**, 133-149.

HERZBERG C.T., FYFE W.S. and CARR M.J. (1983) − *Density constraints on the formation of the continental Moho and crust*. Contrib. Mineral. Petrol., **84**, 1-5.

HILDRETH W. (1981) − *Gradients in silicic magma chambers: implications for lithospheric magmatism*. J. Geophys. Res., **86**, 10153-10192.

HÜBNER J.S. and SATO M. (1970) − *The oxygen fugacity-temperature relationships of manganese oxide and nickel oxide buffers.* Am. Mineral., **55**, 934-952.

JORON J.L., METRICH N., ROSI M., SANTACROCE R. and SBRANA A. (1987) − *Chemistry and petrography: Somma-Vesuvius*. In: Santacroce R. (Ed.), Somma-Vesuvius - Quaderni de "La Ricerca Scientifica", CNR, Roma, **114**, 105-174.

KELEMEN P.B. (1990) − *Reaction between ultramafic rocks and fractionating basaltic magma I. Phase relations, the origin of calc-alkaline magma series, and the formation of discordant dunite.* J. Petrol., **31**, 51-98.

KRETZ, R. (1982) − *Transfer and exchange equilibria in a portion of the pyroxene quadrilateral as deduced from natural and experimental data.* Geochim. Cosmochim. Acta, **46**, 411-422.

KAMESKY V., METRICH N. and CIONI R. (1995) − *Potassic primary melts of Vulsini (Roman Province): evidence from mineralogy and melt inclusions*. Contrib. Mineral. Petrol., **120**, 186-196.

KÖLER T.P. and BREY G.P. (1990) − *Calcium exchange between olivine and clinopyroxene calibrated as a geothermobarometer for natural peridotites from 2 to 60 kbar with applications*. Geochim. Cosmochim. Acta, **54**, 2375-2388.

KRESS V.C. and CARMICHAEL I.S.E. (1991) − *Compressibility of silicate liquids containing Fe_2O_3 and the effect of composition, temperature, oxygen fugacity and pressure on their redox states*. Contrib. Mineral. Petrol., **108**, 82-92.

LE BAS M.J., LE MAITRE R.W., STREKEISEN A. and ZANNETTIN B. (1986) − *A Chemical Classification of Volcanic Rocks based on the Total Alkali-Silica Diagram.* J. Petrol, **27**, 745-750.

LACROIX A. (1907) − Étude *minéralogique des produits silicatés de l'éruption de Vesuve (avril 1906)*. Nouv. Arch. Muséum Paris, **4e** sér., 9.

LACROIX A. (1917) − *Les roches grenues d'un magma leucitique étudiées à l'aide des blocs holocistallins de la Somma*. *Comptes Rendues,* Paris, **165**, 205-216.

LAIOLO M. (2004) − *Petrology of mafic and ultramafic nodules in strombolian and vesuvian lavas and tephra: insights on the genesis of circum-mediterranean magmas.* PhD thesis (in Italian), Università di Torino, 127 pp.

LOUCKS R.R. (1996) − *A precise olivine-augite Mg-Fe-exchange geothermometer.* Contr. Mineral. Petrol., **125**, 140-150.

MARIANELLI P., METRICH N., SANTACROCE R. and SBRANA A. (1995) − *Mafic magma batches at Vesuvius: a glass inclusion approach on the modalities of feeding stratovolcanoes*. Contrib. Mineral. Petrol., **120**, 159-169.

MARIANELLI P., METRICH N. and SBRANA A. (1999) − *Shallow and deep reservoirs involved in magma supply of the 1944 eruption of Vesuvius*. Bull. Volcanol., **61**, 48-63.

MERCIER J.C.C. (1980) − *Single-pyroxene thermobarometry*. Tectonophysics, **70**, 1-37.

MERCIER J.C.C. and NICOLAS A. (1975) − *Textures and fabrics of upper mantle peridotites as illustrated by xenoliths from basalts*. J. Petrol., **16**, 454-487.

MITCHEL R.H. (1986) − *Kimberlites, Mineralogy, Geohemistry and Petrology*. Plenum Press, New York, 442 pp.

NEWTON R.C. CHARLU T.V. and KLEPPA O.J. (1980)

− *Thermochemistry of the high structural state of plagioclase*. Geochim. Cosmochim. Acta, **75**, 369-376.

PECCERILLO A. (1999) − *Multiple mantle metasomatism in central-southern Italy: Geochemical effects, timing and geodynamic implications*. Geology, **27**, 315-318

PONTEVIVO A. and PANZA G.F. (2006) − The Lithosphere-Asthenosphere System in the Calabrian Arc and Surrounding Seas – Southern Italy. Pure Appl. Geophys., **163**, 1617–1659.

RICHET P., BOTTINGA Y., DENIELOU L., PETITET J.P. and TEQUI C. (1982) − *Thermodynamic properties of quartz, crystobalite and amorphous SiO_2: drop calorimetry measurements between 1000 and 1800 °K and a review from 0 to 2000 °K*. Geochim. Cosmochim. Acta, **46**, 2639-2658.

RIGHTER K. and CARMICHAEL I.S.E. (1996) − *Phase equilibria of phlogopite lamphrophyres from western Mexico:biotite-liquid equilibria and P-T estimates for biotite-bearing igneous rocks*. Contrib. Mineral. Petrol., **123**, 1-21.

RITTMANN A. (1933) − *Die geologisch bedingte Evolution und Differentiation des Somma-Vesuvius Magma*. Z. Vulk., **14**, 8-94.

ROBIE, R.A., HEMINGWAY, B.S. and FISHER J.R. (1979) Thermodynamic properties of minerals and related substances at 218.15 K and 1 Bar (105 Pascals) Pressure and Higher Temperatures. USGS Bull., **1452**, 456 pp.

ROEDER P.I.. and EMSLIE R.F. (1970) − *Olivine-liquid equilibrium*. Contrib. Mineral. Petrol., **29**, 275-289.

ROEDER P.L., CAMPBELL I.H. and JAMIESON H.E. (1979) − *A Re-evaluation of the olivine-spinel geothermometer.* Contrib. Mineral. Petrol., **68**, 325-334.

SACK R.O. and GHIORSO M.S. (1989) − *Importance of considerations of mixing properties in establishing an internally consistent thermodynamic database: thermochemistry of minerals in the system* Mg_2SiO_4-Fe_2SiO_4-SiO_2. Contrib. Mineral. Petrol., **102**, 41-68.

SANTACROCE R., BERTAGNINI A., CIVETTA L., LANDI P. and SBRANA A. (1993) − *Eruptive dynamics and petrogenetic processes in a shallow magma reservoir: the 1906 eruption of Vesuvius*. J. Petrol., **34**, 383-425.

SANTACROCE R., CIONI R., MARIANELLI P. and SBRANA A. (2005) – *Understanding Vesuvius and preparing for its next eruption*. In: Balmuth, M. S., Chester D. K. and Johnston, P. A. (Eds.), Cultural Responses to the Volcanic Landscape. The Mediterranean and Beyond. Archaeological Institute of America, Colloquia and Conference Papers, **8**, 27-55.

SAVELLI C. (1967) − *The problem of rock-assimilation of Somma-Vesuvius magma: Composition of Somma and Vesuvius lavas*. Contrib. Mineral. Petrol., **16**, 328-353.

SCANDONE R. and GIACOMELLI L. (1998) – *Vulcanologia. Principi Fisici e Metodi di Indagine*. Liguori Editore, Napoli, 642 pp.

SCHIANO P., CLOCCHIATTI R., OTTOLINI L. and SBRANA A. (2004) − *The relationship between potassic, calc-alkaline and Na-alkaline magmatism in South Italy volcanoes: a melt inclusions approach*. Earth Planet. Sci. Lett., **220**, 121-137.

TRIGILA R. and DE BENEDETTI A. (1993) − *Petrogenesis of Vesuvius historical lavas constrained by Pearce element ratios analysis and experimental phase equilibria*. J. Volcanol. Geotherm. Res., **58**, 315-343.

WASHINGTON H.S. (1906) − *The Roman comagmatic region*. Carnegie. Inst. Publ., **57**, 199 pp

WASHINGTON H.S. (1917) - *The Roman comagmatic region: chemical analyses of igneous rocks*. Prof. Paper, Washington, **99**, 1-120.

WOOD B.J. and TRIGILA R. (2001) − *Experimental determination of aluminous clinopyroxene-melt partition coefficients for potassic liquids, with application to the evolution of the Roman province potassic magmas.* Chem. Geol., **172**, 213-223.

ZAMBONINI F. (1910) − *Mineralogia Vesuviana*. R. Accad. delle Scienze Fisiche e Matematiche, Napoli, 359 pp.

ZOLLO A., GASPARINI P., VIRIEUX J., BIELLA G., BOSCHI E., CAPUANO P., DE FRANCO R., DELL'AVERSANA P., DE NATALE G., DE MATTEIS R., IANNACONE G., GUERRA I., LE MEUR H. and MIRABILE I. (1998) − *An image of Mt. Vesuvius obtained by 2D seismic tomography*. J. Volcanol. Geotherm. Res., **82**, 161-163.